Journal of ELECTRONIC MATERIALS, Vol. 48, No. 6, 2019
https://doi.org/10.1007/s11664-019-07136-3

Metastable δ-Fe During Reduction of Ferric Oxide and Its Magnetic Properties

S.B. QADRI,[1,2] B.-T. FAHED,[1] E.P. GORZKOWSKI,[1] B.B. RATH,[1] K. BUSSMANN,[1] and J. FENG[1]

1.—U. S. Naval Research Laboratory, Washington, DC 20375, USA. 2.—e-mail: syed.qadri@nrl.navy.mil

Metallic iron exhibits three distinct crystallographic phases, α-(bcc), γ-(fcc), and δ-(bcc), under variable temperature. In this paper, we show that iron oxide, in the hematite composition, Fe_2O_3, was reduced to its pure metallic form, using carbon obtained from the nut shells of pistachios or walnuts, at temperatures exceeding 1400°C, annealed in argon gas atmosphere. In addition to α-, γ-, and δ-phases of Fe, x-ray diffraction analysis shows the presence of carbon nanotubes (CNTs) and amorphous carbon. There was no residual ferric oxide present as long as the appropriate ratios of nut shell powder to Fe_2O_3 were selected. The quantity of each of the three Fe phases was a function of the temperature and the time of processing. Transmission electron microcopy revealed the presence of large quantities of CNTs formed during annealing. Magnetic data suggested the average magnetic moment was consistent with α-Fe, but reduced moment for both the γ-Fe and δ-Fe. This is the first observation of producing δ-Fe stable at room temperature along with CNTs. This has potential industrial applications as composites. Although both α- and δ-ferrites are body-centered cubic, δ-ferrite is a more compact structure indicative of higher specific density and hence improved mechanical properties. In addition, the magnetic and structural properties of the metastable Fe provide insights in understanding the novel properties of artificial structures on the nanometer scale made using advanced thin film techniques.

Key words: Carbon nanotubes, metastable phase, magnetic materials, x-ray diffraction

INTRODUCTION

Iron, which is a transition metal on the periodic table, is one of the most abundant elements present in both the earth's outer and inner core. It has multitudes of applications due to its magnetic properties, wear and corrosion resistance, high strength and toughness in several industries, such as automotive, gas transport and power generation, high strength alloys for industrial applications, along with for many biological and medical applications. Iron metal is produced on a commercial scale from iron ore (ferric oxide) by a high temperature reduction process in a blast furnace, where the ore is reduced using carbon sources into metallic Fe with high carbon content. The excessive carbon content is removed in an open hearth furnace in oxygen atmosphere to produce a required alloying element needed for a wide range of steel.

There are many agricultural residues, among which contain silica and organic matter such as rice husk, wheat husk, corn husk, sorghum leaves and peanut shells. Other residues that contain mostly carbonaceous matter are nut shells such as almonds, walnuts, pistachios, coconuts, macadamias, and cashews. In our previous studies, we demonstrated the synthesis of SiO_2, SiC, Si_3N_4, and zinc silicate by pyrolizing these residues in air,

(Received September 14, 2018; accepted March 12, 2019; published online March 22, 2019)

argon or in nitrogen atmospheres.[1–6] Moreover, we showed that the agriculture residue that contains only organic matter without any significant silica content can be used in reduction of metal oxides to metals and in some cases metals in the presence of carbon nanotubes (CNTs).[7] In our previous studies of reduction of Fe_2O_3 to metal Fe using coconut shells, we showed the formation of γ-Fe and α-Fe phases. However, in contrast to coconut shells where the formation of SiC was reported, the nut shells of almonds, walnuts, pistachios, macadamias, and cashews have only carbonaceous matter and fewer impurities such as Si and Ca.[8,9] Large quantities of these agriculture residues, which are considered waste products, are available and, therefore, can be effectively made use of in the synthesis of important materials that will have significant industrial impact.

Iron forms many crystallographic phases when subjected to varying thermodynamics conditions of temperature and pressure.[10,11] Under standard conditions of pressure and temperature, iron exists in a body-centered cubic (bcc) crystal structure (α-Fe) up to a temperature of 911°C, in a close-packed face-centered cubic (fcc) structure (γ-Fe) between 911°C and 1392°C and finally in a high-temperature bcc phase (δ-Fe) above 1392°C until 1538°C (the melting point), respectively. Thus, δ-Fe and α-Fe, which are both bcc phases of iron, are considered distinct forms due to their stability in different temperature ranges and their different lattice parameters. The δ phase is rarely seen at room temperature except in certain alloys of iron containing high concentrations of Cr, Ni, Mo and Mn.[12] These phases of iron dissolve varying percentages of carbon, 0.021% for α-Fe and up to 2.04% for γ-Fe. In addition, carbon nanotubes have unique electronic, magnetic and mechanical properties and are at least orders of magnitude stronger than steel and yet very light in weight. Therefore, addition of carbon nanotubes to Fe could reinforce or enhance its mechanical properties.

The present study demonstrates a more efficient and cost-effective way of utilizing nut shells as a carbon source (as an illustration, pistachio and walnut used in this study) mixed in the appropriate ratio with Fe_2O_3 (hematite) to produce metastable phases of Fe along with copious amounts of carbon nanotubes. In addition, for the first time we observed the formation of a metastable δ-Fe phase that is stable at room temperature and have demonstrated its ferromagnetic characteristics.

EXPERIMENTAL DETAILS

Samples consisting of Fe_2O_3 and powdered pistachio shells were prepared by ball milling with an SPEX 8000 M including stainless steel milling media. The samples were thoroughly mixed and then ball-milled to obtain a uniform homogenous powder. The powder was packed in a die to produce 1-cm diameter disks with a 2.5–3-mm depth, and a hydraulic press was used to form the pellets. The pellets were thermally treated in a standard tube furnace at temperatures exceeding 1400°C for an interval of 4–6 h in an argon atmosphere. The samples were cooled down to room temperature and their XRD scans were taken using a Rigaku 18 kW rotating anode generator with a copper target and a high resolution powder diffractometer. The x-ray diffraction profiles were collected using monochromatic CuKα radiation. Samples for TEM analysis were prepared by mixing the pyrolyzed sample with ethyl alcohol to form a colloidal solution in an ultrasonic cleaner. A carbon covered 200 mesh copper grid was subsequently submerged into the mixture to collect Fe and CNTs. A FEI Tecnai G2 TEM was used to study the sample at 300 kV.

RESULTS AND DISCUSSION

The x-ray fluorescence spectrum of the pistachio pellet is presented in Fig. 1, and it shows the presence of trace amounts of K, Ca, Fe, Cr, Mn, Cu and Zn. A composite figure of diffraction profiles taken from a sample consisting of pistachio powder mixed with Fe_2O_3 in a weight ratio of 1:0.05 and a sample heat treated sample at 1600°C is given in Fig. 2. The data for the untreated sample consist of x-ray diffraction peaks corresponding to α-Fe_2O_3 and broad peak characteristics of amorphous material originating from the pistachio powder. The diffraction peaks corresponding to Fe_2O_3 have been indexed based on $R\,\bar{3}c$ rhombohedral phase, and a Rietveld analysis of the whole diffraction profile gave lattice parameters $a = 5.039$ Å and $c = 13.740$ Å, which are in agreement with the published values.[13] The diffraction scan from the sample treated at 1600°C shows peaks that are indexed based on 2H-graphite phase and the BCC δ-Fe phase. Figure 3 is a composite of the x-ray diffraction scans taken from samples heat treated at 1400°C, 1500°C, and 1600°C. The scans for 1400°C

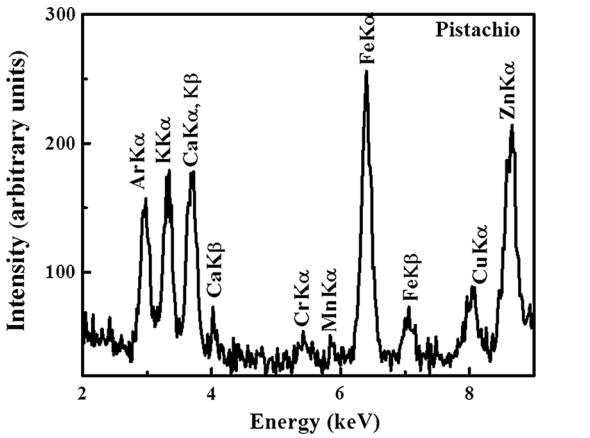

Fig. 1. Energy dispersive x-ray fluorescence of pistachio powder showing trace amounts of K, Ca, Cr, Mn, Fe, Cu, and Zn.

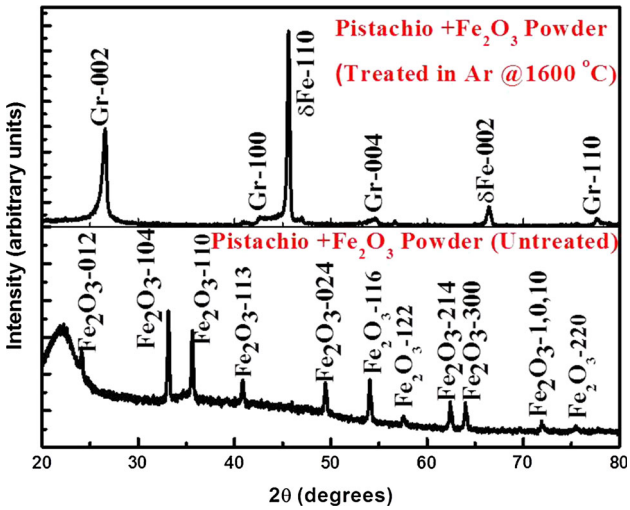

Fig. 2. Comparison of XRD patterns of mixed pistachio powder with Fe_2O_3 showing peaks corresponding to α-phase of Fe_2O_3 with the sample heat treated at 1600°C showing peaks corresponding to only δ-phase of Fe and 2H-graphite peaks (CNTs).

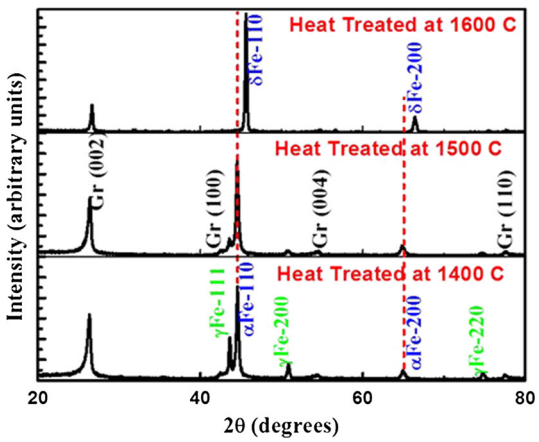

Fig. 3. Comparison of XRD pattern samples heat treated at 1400°C, 1500°C, and 1600°C. The XRD scans for samples heat treated at 1400°C and 1500°C show mixed α- and γ-Fe phases and only δ-phase of Fe for the sample at 1600°C.

and 1500°C show peaks of the mixed phases of austenite (γ-phase) and α-Fe in addition to peaks corresponding to graphite 2H-phase (CNTs). In order to distinguish between α- and δ-Fe phases, a vertical dashed line is drawn that shows how the bcc peaks (110) and (200) have shifted towards high 2θ values for δ-Fe. Both α- and δ-Fe phases are bcc phases and the only difference is in the lattice parameters. The α-Fe has a lattice parameter of 2.866 Å, whereas δ-Fe has a lattice parameter of 2.82 Å. All the diffraction scans were analyzed using Rietveld whole profile analysis to obtain quantitative weight percentages of each phase of Fe along with CNTs.

A TEM micrograph for the sample processed at 1500°C is given in Fig. 4 showing a large volume

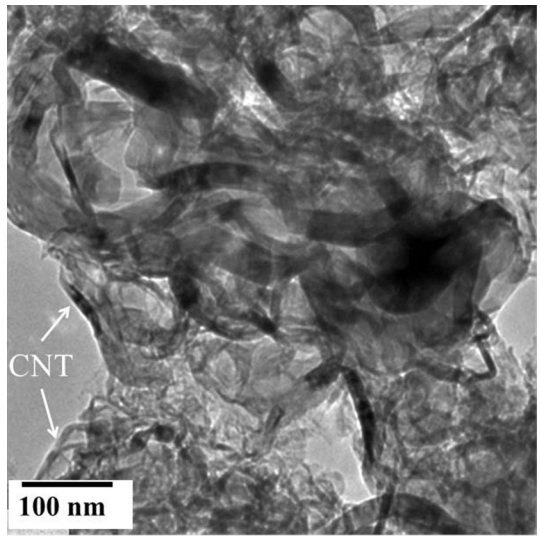

Fig. 4. TEM micrographs of samples annealed at 1500°C for 4 h in Ar atmosphere revealing the presence of CNTs.

percentage of CNTs. All three samples showed the presence of large quantities of CNTs. Based on the Rietveld quantitative analysis of x-ray diffraction profiles and knowing the starting Fe content, the mass of the CNTs is calculated to be approximately 0.14 g for starting 1 g of pistachio nut powder.

The magnetic measurements, M versus H curves for the three samples are given in Fig. 5a, b and c. The saturation magnetization for 1500°C sample is reduced compared to the one at 1400°C sample. Based on the x-ray measurements the 1400°C sample consists of 87% α-Fe and 13% γ-Fe (crystallite size for α-35 nm and γ-57 nm), whereas 1500°C 73% α-Fe and 27% γ-Fe (crystallite size for α-31 nm and γ-28 nm). The data was normalized using the mass of the Fe present in the samples. However, the moments for each phase were determined by using the weight % of each phase from x-ray Rietveld analysis and using the measured saturation moment. The results show the moments to be 220 emu/g or 2.20 μ_B for α-phase and 77 emu/g or 0.77 μ_B for the γ-Fe phase. These measurements suggest γ-Fe to be ferromagnetic with a low moment of 0.77 μ_B. On the other hand the sample treated at 1600°C shows only the presence of only δ-Fe with a lattice parameter of 2.82 Å (crystallite size 40 nm). The magnetic data suggested this phase to be ferromagnetic with a moment of 162 emu/g or 1.62 μ_B , which is a reduced value compared to that for α-Fe.

The theoretical model predicted that the fcc γ-Fe can have three magnetic phases including non-magnetic, an antiferromagnetic state, and low and high moment in the ferromagnetic state.[14,15] Based on by extrapolation of high temperature data, the lattice parameter for the fcc phase is expected to be 3.59 Å. Our measurements showed a lattice parameter with 3.585 Å with a low moment of 0.77 μ_B in agreement with the theoretical predictions. On the other hand, it was reported that the magnetic

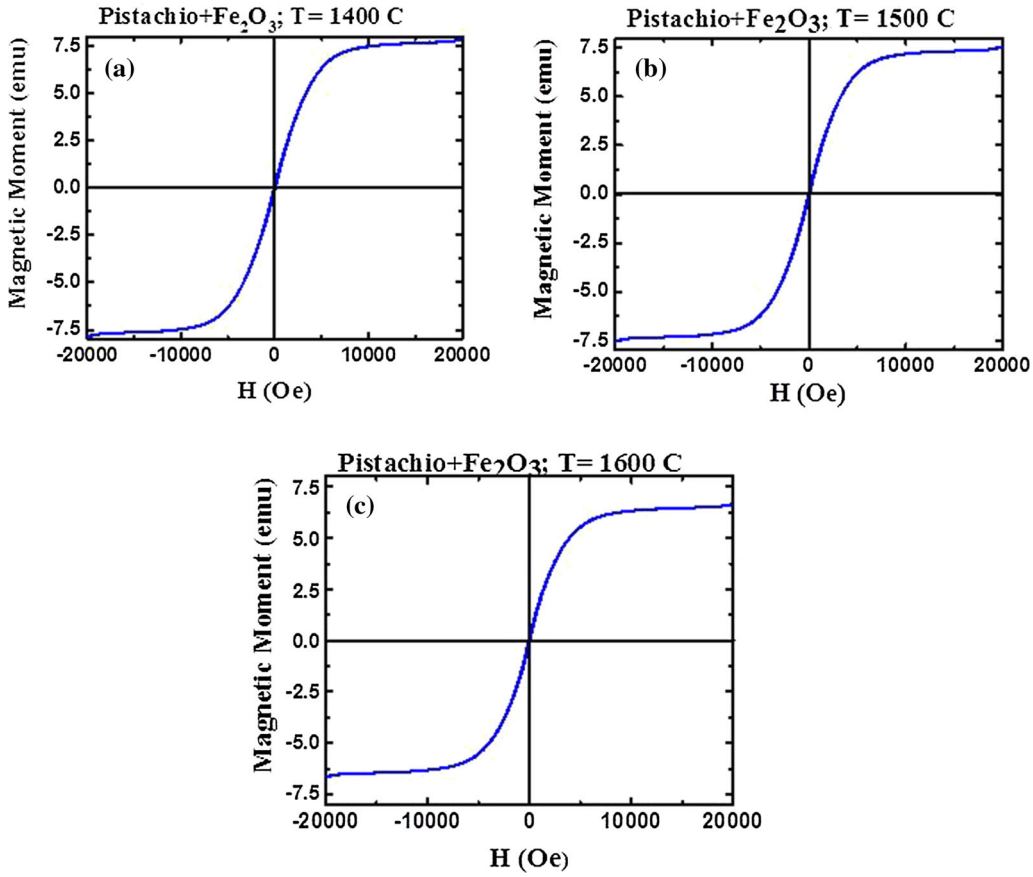

Fig. 5. M versus H curves for samples (a) heat treated at 1400°C (87% α-Fe and 13% γ-Fe), (b) heat treated at 1500°C (73% α-Fe and 27% γ-Fe), and (c) heat treated at 1600°C (only δ-Fe) showing that the saturation magnetization decreased for 1600°C sample.

moments of epitaxially grown thin Fe films on GaAs (110) substrates showed significant reduction in magnetic moment although it was not identified as δ-Fe. In the synthesis of novel artificial structures on the nanometer scale using sophisticated thin-film techniques, the prospects have opened for inducing metastable structures with new, perhaps exotic, properties. Recently, spintronics research has been focused in making superlattice structures involving Fe as one of the thin magnetic layer. It has been reported that the reduced magnetic moment of Fe to be reduced when compared to the bulk α-Fe phase and the lattice parameters to be reduced.[16,17] The present research on δ-Fe provides an insight into the observed electronic and magnetic properties of such systems.

CONCLUSIONS

Pure pistachio shells when heat treated above 1400°C in argon atmosphere formed only amorphous carbon. Pistachio nut shells mixed with Fe_2O_3 when heat treated in argon atmosphere at 1400°C and 1500°C resulted in the formation of pure α- and γ-Fe phases with large quantities of CNTs. When the sample of pistachio mixed with Fe_2O_3 was heated to 1600°C and then cooled to room temperature resulted in pure δ-Fe phase, commonly not seen in iron, along with large quantities of CNTs. Magnetic data showed α-Fe to have magnetic moment of 220 emu/g or 2.2 μ_B whereas the γ-Fe to be ferromagnetic with a moment of 77 emu/g or 0.77 μ_B and δ-Fe with 162 emu/g or 1.62 μ_B. Both δ- and γ-Fe have reduced moments when compared to α-Fe phase. In conclusion, for the first time we observed the formation of metastable δ-Fe phase, stable at room temperature and have demonstrated its ferromagnetic characteristics.

REFERENCES

1. S.B. Qadri, E.P. Gorzkowski, B.B. Rath, J. Feng, S.N. Qadri, H. Kim, and M.A. Imam, *J. Appl. Phys.* 117, 044306 (2015).
2. S.B. Qadri, B.B. Rath, E.P. Gorzkowski, J. Wollmershauser, and C. Feng, *J. Appl. Phys.* 118, 104904 (2015).
3. S.B. Qadri, M. Imam, A. Fliflet, B.B. Rath, R. Goswami, and J. Caldwell, *J. Appl. Phys.* 111, 073523 (2012).
4. S.B. Qadri, E.P. Gorzkowski, B.B. Rath, C.R. Feng, R. Amarasinghe, J.A. Freitas Jr, J.C. Culbertson, and J.A. Wollmershauser, *J. Cryst. Growth* 476, 25 (2017).
5. S.B. Qadri, E.P. Gorzkowski, B.B. Rath, C.R. Feng, and R. Amarasinghe, *J. Alloys Compd.* 708, 67 (2017).
6. S.B. Qadri, E.P. Gorzkowski, B.B. Rath, C.R. Feng, and R. Amarasinghe, *AIP Adv.* 6, 115204 (2016).
7. S.B. Qadri, E.P. Gorzkowski, K. Bussmann, B.B. Rath, and J. Feng, *AIP Adv.* 8, 055134 (2018).

8. A. Selvam, N.G. Nair, and P. Singh, *J. Mater. Sci. Lett.* 17, 57 (1998).
9. R. Araga and C.S. Sharma, *Mater. Lett.* 188, 205 (2017).
10. N. Gunkelmann, E.M. Bringa, K. Kang, G.J. Ackland, C.J. Ruestes, and H.M. Urbassek, *Phys. Rev. B* 86, 144111 (2012).
11. T. Lee, M.I. Baskes, S.M. Valone, and J.D. Doll, *J. Phys. Condens. Matter* 24, 225404 (2012).
12. H.C. Vacher and C.J. Bechtoldt, *J. Res. NBS* 53, 2517 (1954).
13. E. Wolska and U. Schwertman, *Z. Kristallogr.* 189, 223 (1989).
14. C.S. Wang, B.M. Klein, and H. Krakauer, *Phys. Rev. Lett.* 54, 1852 (1985).
15. A.S. Edelstein, C. Kim, S.B. Qadri, K.H. Kim, V. Browning, H.Y. Yu, B. Maruyama, and R.K. Everett, *Solid State Commun.* 76, 1379 (1990).
16. S.B. Qadri, M. Goldenberg, G.A. Prinz, and J.M. Ferrari, *J. Vac. Sci. Technol. B* 3, 718 (1985).
17. J.J. Krebs, B.T. Jonker, and G.A. Prinz, *J. Appl. Phys.* 61, 2596 (1987).